



**HAL**  
open science

## High resolution far-infrared synchrotron spectroscopy of 2-furfural conformers: Fundamental and hot bands

Sathapana Chawananon, Manuel Goubet, Olivier Pirali, Robert Georges, Anthony Roucou, Ikram Hadj Said, Maria Luisa Senent, A. Cuisset, Pierre Asselin

### ► To cite this version:

Sathapana Chawananon, Manuel Goubet, Olivier Pirali, Robert Georges, Anthony Roucou, et al.. High resolution far-infrared synchrotron spectroscopy of 2-furfural conformers: Fundamental and hot bands. *The Journal of Chemical Physics*, 2024, 161 (1), pp.014308. 10.1063/5.0213834 . hal-04649822

**HAL Id: hal-04649822**

**<https://hal.science/hal-04649822>**

Submitted on 19 Jul 2024

**HAL** is a multi-disciplinary open access archive for the deposit and dissemination of scientific research documents, whether they are published or not. The documents may come from teaching and research institutions in France or abroad, or from public or private research centers.

L'archive ouverte pluridisciplinaire **HAL**, est destinée au dépôt et à la diffusion de documents scientifiques de niveau recherche, publiés ou non, émanant des établissements d'enseignement et de recherche français ou étrangers, des laboratoires publics ou privés.



Distributed under a Creative Commons Attribution - NonCommercial 4.0 International License

# High resolution far-Infrared synchrotron spectroscopy of 2-furfural conformers: fundamental and hot bands

Sathapana Chawananon<sup>1</sup>, Manuel Goubet<sup>2</sup>, Olivier Pirali<sup>3</sup>, Robert Georges<sup>4</sup>, Anthony Roucou<sup>5</sup>, Ikram Hadj Said<sup>6,7</sup>, María Luisa Senent<sup>7</sup>, Arnaud Cuisset<sup>5</sup> and Pierre Asselin<sup>1\*</sup>

<sup>1</sup>Sorbonne Université, CNRS, MONARIS, UMR 8233, 4 place Jussieu, Paris, F-75005 France.

<sup>2</sup>Université de Lille, CNRS, UMR 8523 - PhLAM - Physique des Lasers Atomes et Molécules, F-59000 Lille, France.

<sup>3</sup>Université de Paris-Saclay, CNRS, Institut des Sciences Moléculaires d'Orsay, F-91405 Orsay, France

<sup>4</sup>Université de Rennes, CNRS, IPR (Institut de Physique de Rennes)—UMR 6251, F-35000 Rennes, France

<sup>5</sup>Université du Littoral Côte d'Opale, UR4493, LPCA, Laboratoire de Physico-Chimie de l'Atmosphère, F-59140 Dunkerque, France

<sup>6</sup>USTHB, Laboratory of Thermodynamics and Molecular Modeling, Faculty of Chemistry, BP32, El Alia, 16111, Bab Ezzouar, Algiers, Algeria.

<sup>7</sup>Departamento de Química y Física Teóricas, Instituto de Estructura de la Materia, IEM-CSIC, Serrano121, Madrid 28006; Unidad Asociada GIFMAN, CSIC-UHU, Spain.

## Abstract

In the continuity of a previous jet-cooled rovibrational study of *trans*- and *cis*- conformers of 2-furfural in the mid-infrared region (700-1750 cm<sup>-1</sup>) [Chawananon *et al*, *Molecules* **28** (10), 4165 (2023)], the present work investigates the far-infrared spectroscopy of 2-furfural using a long path absorption cell coupled to a high-resolution Fourier transform spectrometer and synchrotron radiation at the AILES beamline of the SOLEIL synchrotron. Guided by anharmonic calculations, vibrational energy levels and excited-state rotational constants are sufficiently predictive for a complete assignment of all fundamental and combination bands up to 700 cm<sup>-1</sup>, as well as the rovibrational analysis of 4 (1) low-frequency modes of *trans*- (*cis*-) 2-furfural. A global rovibrational simulation, including far-infrared rovibrational lines and microwave and millimetre-wave rotational lines assigned in a previous study by [Motiyenko *et al*, *J. Mol. Spectrosc.*, **244**, 9 (2007)], provides a reliable set of ground- and excited-state rotational parameters involving ring torsion, bending and ring puckering modes of 2-furfural. In a second step, a rovibrational analysis of several hot band sequences, mainly involving the lowest frequency ring CHO torsion mode, is carried out. Reliable values of some anharmonic coefficients are obtained experimentally, and could serve as a benchmark for validating advanced anharmonic calculations related to these large amplitude motions of flexible molecules.

## I- Introduction

Furan and its related compounds are primary and secondary pollutants in the atmosphere; they are involved in the formation of atmospheric particles such as secondary organic aerosols (SOAs).<sup>1</sup> Among them, furfural (FF), an oxygenated five-membered aromatic molecule (C<sub>5</sub>H<sub>4</sub>O<sub>2</sub>) is produced by biomass combustion mainly from the pyrolysis of hemi-cellulose.<sup>2</sup> Besides identifying the chemical composition of biomass burning emissions<sup>3</sup> and the compounds involved in the SOAs formation along with their main precursors,<sup>4</sup> there is a fundamental interest in monitoring these molecules. Currently, the LPCA group has studied in the CHARME (CHamber for the Atmospheric Reactivity and the

---

\*Corresponding author (email :pierre.asselin@sorbonne-universite.fr)

**Metrology of the Environment**) simulation chamber the reactivity of furans with day time and night time major oxidants, respectively OH and NO<sub>3</sub>. **These measurements clearly demonstrated that the gas-phase oxidation products of FF such as methylfurans contribute significantly to the SOA formation, while FF alone is not efficient.**<sup>5</sup> *In situ* monitoring of furan derivatives during the oxidation processes will be the next step<sup>6</sup>, but it requires knowledge of their rovibrational signatures through high-resolution experiments over a broad spectral range.

Previous spectroscopic investigations of FF in the gas phase have focused on the ortho isomer (2-FF). Little *et al.* exploited low-resolution Fourier transform (FT) spectra in the far-infrared (far-IR) to determine the relative stability between *trans* and *cis* conformers.<sup>7</sup> Based on the modeling of an asymmetric torsional potential function, the energy difference between the two conformations is estimated to 3.42(29) kJ/mol and the conformational barrier height to 38.94(24) kJ/mol, meaning that neither observable splitting due to quantum tunneling nor relaxation in the supersonic jet is expected. In the mid-IR range, Johnson *et al.* have exploited medium-resolution FTIR measurements (0.112 cm<sup>-1</sup>) to derive the vibrational cross-sections available in the atmospheric and specific HITRAN/PNNL databases dedicated to quantitative IR spectroscopy of gases emitted by biomass burning.<sup>8</sup> High-resolution analyses of the ground state of the *trans* and *cis* conformers and of the lowest-energy torsional state for the most stable *trans*-2-FF were performed using jet-cooled Fourier transform microwave spectroscopy (FTMW).<sup>9</sup> Motiyenko *et al.* extended the analysis of these conformers in the millimeter-wave (mmW) region at room temperature, providing molecular parameters for all the low-lying vibrational states up to 400 cm<sup>-1</sup>.<sup>10</sup>

The present work is a follow up of our recent high-resolution study of 2-FF in the mid-IR region using two complementary jet-cooled spectroscopic setups.<sup>11</sup> The aims of this previous work were twofold. In a first step, rovibrational spectra recorded at low rotational temperatures were exploited to derive reliable excited state molecular parameters of *trans*- and *cis*-2-FF vibrational bands in the fingerprint region between 700 and 1800 cm<sup>-1</sup>. In a second step, the medium-resolution spectrum of 2-FF recorded at 298.15 K available in the HITRAN<sup>12</sup> database was reconstructed by extrapolating the data obtained from our low-temperature analyses, highlighting the strong contribution of hot bands in the room temperature contour of 2-FF vibrational band spectra, estimated to about 50 % of the fundamental band.

Our objective here is to investigate in detail the high-resolution far-IR spectrum of 2-FF recorded in a long-path absorption cell at room temperature. Building on previous microwave measurements by Motiyenko *et al.*,<sup>9-10</sup> the present rovibrational analysis aims to refine the existing set of molecular parameters of the excited state of 2-FF by extending the study to the most intense fundamental vibrations below 600 cm<sup>-1</sup>, in particular the ring-CHO torsion ( $\nu_{27}$ ), the ring-CHO in-plane and out-of-plane bending (respectively  $\nu_{19}$  and  $\nu_{26}$ ) and ring puckering ( $\nu_{25}$ ) modes. We will then proceed to the vibrational assignment and rovibrational analysis of the hot band patterns related to most of these fundamentals in order to extract reliable values of the anharmonic coefficients  $\chi_{i,j}$ , probably involving the lowest frequency  $\nu_{27}$  torsional mode due to its larger vibrational population at 300 K. The predictive power of theoretical calculations on these large aromatic molecules will be discussed in the light of comparisons with experimental molecular parameters, vibrational energy levels and anharmonic coefficients.

## II- Methods

### II-1 Fourier transform infrared experiment

Gas-phase 2-furfural (> 99 %, Aldrich) was injected into a room-temperature multipass cell equipped with 50  $\mu\text{m}$ -thick propylene films as cell windows, for which the optics of the White-type cell were adjusted to obtain an absorption path of about 150 m long. Four fundamental low-frequency bands of *trans*-2-FF ( $\nu_{27}$ ,  $\nu_{26}$ ,  $\nu_{25}$  of c-type and  $\nu_{19}$  of a/b-type) and three bands of *cis*-2-FF ( $\nu_{19}$ ,  $\nu_{26}$  and  $\nu_{25}$ ), for which the intensities calculated in the harmonic approximation are all between 5 and 13 km/mol, could be observed in the 120-620  $\text{cm}^{-1}$  spectral range. The gas pressure was about 20  $\mu\text{bar}$  to maximize the absorption signal without reaching saturation of the intense Q branches of the c-type bands. The far-IR spectrum of 2-FF was recorded using the SOLEIL synchrotron radiation extracted by the AILES beamline as a continuum source of the FT interferometer equipped with a He-cooled bolometer detector and a 6  $\mu\text{m}$  mylar beamsplitter.<sup>13</sup> An acquisition time of 19 hours, corresponding to the coaddition of 380 scans recorded at the ultimate resolution of 0.001  $\text{cm}^{-1}$ , was required to obtain a sufficient SNR to undertake the successful rovibrational analysis of these weak bands. The entire spectrum was calibrated using the remaining far-IR water absorption lines.<sup>14</sup> Thanks to the high SNR of the far-IR spectrum, line position accuracy was estimated to be about 0.0002  $\text{cm}^{-1}$  for the rovibrational lines of four most intense fundamentals observed. For the three other less intense bands observed in this range, no rovibrational analysis could be carried out.

### II-2- Electronic structure calculations

To obtain reliable rotational constants, the equilibrium structures of *trans*- and *cis*-2-furfural have been calculated using explicitly correlated coupled cluster theory with single and double substitutions augmented by a perturbative treatment of triple excitations, (CCSD(T)-F12)<sup>15,16</sup> as it is implemented in MOLPRO version 2022<sup>17</sup> and using the default options. The procedure was applied in connection to the cc-pCVTZ-F12 basis set<sup>18</sup> (denoted in this paper by CVTZ-F12) optimized for accurately describing core-core and core-valence correlation effects. All the electrons were correlated in the post-SCF process.

Anharmonic frequencies and the anharmonic contribution to the rotational constants were obtained using vibrational second order perturbation theory (VPT2)<sup>19</sup> implemented in GAUSSIAN 16 version C.01<sup>20</sup>. The force field was computed with second order Möller-Plesset theory (MP2)<sup>21</sup> in connection with the aug-cc-pVTZ basis set (denoted in this paper as AVTZ)<sup>22</sup>.

The rotational constants were computed in the ground vibrational state and in the first excited vibrational energy levels using the equation:

$$B_v = B_e(\text{CCSD(T)-F12/CVTZ-F12}) + \Delta B^{\text{vib}}(\text{MP2/AVTZ}) \quad (1)$$

The vibrational contribution  $\Delta B^{\text{vib}}$  was determined from the VPT2  $\alpha_r^i$  vibration-rotation interaction parameters and the MP2/AVTZ cubic force field.

Preliminary results of the anharmonic fundamentals and ground vibrational rotational constants were performed at different levels of theory using *ab initio* calculations with different basis sets or Density Functional Theory with different functionals including Grimme's dispersion correction.<sup>23,24</sup>

A variational procedure of reduced dimensionality was employed to explore the large amplitude motions (LAMs) involving the COH group. Details of this procedure can be found in previous papers.<sup>25</sup>

## III Results

### III-1 Vibrational analysis

Fig.1a displays an overview of the high-resolution far-IR spectrum of *trans*-2-FF. The contours of the fundamental bands  $\nu_{27}$ ,  $\nu_{19}$ ,  $\nu_{26}$ , and  $\nu_{25}$  are clearly observed. The characteristic intense Q branches for the *c*-type bands  $\nu_{27}$ ,  $\nu_{26}$  and  $\nu_{25}$  have origins centered at 146.20, 235.82 and 595.98  $\text{cm}^{-1}$ . For the hybrid *a/b*-type band  $\nu_{19}$ , the origin of the Q branch is expected at 203.13  $\text{cm}^{-1}$ . As well, the experimental intensities of four bands well agree with the calculated 6/6/9/11 ratio of anharmonic intensities. Three weaker bands are also observed at 462.3, 622.6 and 694.3  $\text{cm}^{-1}$  (Fig.1a), two of which may correspond to as yet unassigned fundamental bands, such as  $\nu_{18}$  and  $\nu_{24}$ , calculated at 492 and 635  $\text{cm}^{-1}$ , respectively. Their contours, *b*-type for the band at 462.3  $\text{cm}^{-1}$  and *c*-type for that at 622.6  $\text{cm}^{-1}$ , are fully compatible with the calculated dipole moment orientations, confirming our assignment. With  $\nu_{18}$  at 462.3  $\text{cm}^{-1}$ , the band at 694.3  $\text{cm}^{-1}$  may correspond to the *c*-type combination band ( $\nu_{18} + \nu_{26}$ ) with an anharmonic coefficient  $\chi_{18,26}$  equal to around -3.8  $\text{cm}^{-1}$ . Consequently, the 6 lowest frequency fundamental bands of *trans*-2-FF are observed and assigned (Table 1) on the basis of anharmonic predictions.

While three fundamental bands of *cis*-2-FF have intensities comparable to those of the *trans*-conformer, its lower relative stability, which corresponds to a *trans/cis* ratio equal to 3/1 at room temperature for an energy difference of 286  $\text{cm}^{-1}$ , makes their observations more challenging. Only the  $\nu_{26}$  band (13  $\text{km/mol}$ , calculated value: 285  $\text{cm}^{-1}$ ) is clearly observed at 280.3  $\text{cm}^{-1}$  (Fig. 1b), largely shifted from the *trans*  $\nu_{26}$  band ( $\sim 45 \text{ cm}^{-1}$ ), as the CHO-ring out-of-plane bending motion is highly conformer-sensitive, thus facilitating their respective rovibrational analyses. Conversely, the  $\nu_{25}$  *cis* band, predicted to be very close (less than 1  $\text{cm}^{-1}$ ) to the *trans* band, could be unambiguously assigned at 595.9  $\text{cm}^{-1}$  once the  $\nu_{25}$  *trans* band was fully analyzed. The full list of far-IR vibrational bands observed for both conformers, together with band center frequencies compared with low-resolution vibrational measurements of Ref. [10] and anharmonic vibrational energy levels calculated with MP2/AVTZ, are reported in Table 1.

Hot bands involving the lowest frequency modes  $\nu_{27}$ ,  $\nu_{19}$ ,  $\nu_{26}$  are expected in the room temperature spectrum. These features, all red-shifted relative to the fundamental bands  $\nu_{27}$ ,  $\nu_{26}$ , and  $\nu_{25}$ , were observed in the low-J region of the P branches (Fig. 1). The different observed hot band sequences are vibrationally assigned as following:  $(n + 1)\nu_{27} \leftarrow n\nu_{27}$  up to  $n = 4$ ;  $(n + 1)\nu_{26} \leftarrow n\nu_{26}$  up to  $n = 2$ ,  $\nu_{26} + n\nu_{27} \leftarrow \nu_{26}$  up to  $n = 4$ ;  $\nu_{25} + n\nu_{27} \leftarrow \nu_{25}$  up to  $n = 3$ . Thanks to the vibrational assignment of overtones ( $n\nu_i$ ) and combinations ( $n\nu_i + \nu_j$ ), an updated version of the energy level scheme for both conformers could be performed and is displayed in Fig. 2. Their partial rovibrational analyses will be presented in section III-3.

### III-2 Rovibrational analysis

Our rovibrational analyses of 2-FF in the far-IR range are guided by previous MW and mmW studies by Motiyenko *et al.* in the 7-21 GHz and 49-330 GHz ranges.<sup>9,10</sup> The ground state (GS) and excited states (ES) of *trans*-2-FF and *cis*-2-FF up to 470  $\text{cm}^{-1}$  have been assigned and analyzed, in particular for the three lowest frequency vibrational bands,  $\nu_{27}$ ,  $\nu_{19}$  and  $\nu_{26}$ . Accurate values of rotational and quartic centrifugal distortion (CD) constants were determined for these fundamental bands, requiring in most cases the introduction of several sextic and octic parameters to reproduce the data within experimental accuracy. In order to limit the number of adjustable parameters, the present

far-IR study of the two furfural conformers aims to perform a global fit for each conformer that will include all the GS and 3 lowest ES rotational lines for *trans*- and *cis*-2-FF and all the rovibrational lines of  $\nu_{27}=1$ ,  $\nu_{19}=1$ ,  $\nu_{26}=1$ , and  $\nu_{25}=1$  (bands noted hereafter  $\nu_{27t}$ ,  $\nu_{19t}$ ,  $\nu_{26t}$ , and  $\nu_{25t}$ ) for *trans*-2-FF and  $\nu_{26}=1$  (band noted hereafter  $\nu_{26c}$ ) for *cis*-2-FF.

Initially, rovibrational analyses of each fundamental band were performed separately, starting with the ES parameters of Motiyenko *et al.*<sup>10</sup> The fundamental band of each conformer is fitted with the PGOPHER program<sup>26</sup> using a Watson-type semirigid model for asymmetric tops (*a* reduction in the  $I_r$  representation) developed up to octic CD terms. Global fits of GS+4ES<sub>t</sub> for the *trans* conformer and GS+1ES<sub>c</sub> for the *cis* conformer are performed with the SPFIT/SPCAT programs<sup>27</sup> by first fixing the GS constants and then progressively releasing them. A total of 18540 (4113) rovibrational lines and 3935 (3353) rotational lines of *trans*-2-FF (*cis*-2-FF), respectively, were fitted within experimental accuracy with a root mean square (RMS) value of 8 kHz for MW and mmW lines and 0.00015 cm<sup>-1</sup> for IR lines. Except for the  $\nu_{25}$  band, for which the rovibrational lines were fitted using up to quartic CD constants only, the three lowest frequency bands were fitted with sextic CD constants and at least one octic constant. Figures 3 to 7 display the comparison between experimental far-R spectra of  $\nu_{27t}$ ,  $\nu_{19t}$ ,  $\nu_{26t}$ ,  $\nu_{26c}$  and  $\nu_{25t}$ , respectively, and the simulations of the asymmetric top band contour of the fundamental band alone. The band centers, ground-state and upper-state rotational parameters of the two conformers are shown in Tables 2 and 3. Tables S1 and S2 (SupMat1) include line assignments, measured frequencies, uncertainties and deviations for *trans*- and *cis*-2-FF. For future experiments, the complete set of calculated rovibrational transitions obtained with SPCAT program is presented for *cis*- and *trans*- conformers (SupMat2-*cis*, SupMat3-*trans*).

### III-3 Hot band analyses

The rotational structure of hot-band transitions observed on the red side of Q branches of  $\nu_{27t}$ ,  $\nu_{26t}$ ,  $\nu_{26c}$  and  $\nu_{25t}$  bands was exploited to derive accurate  $\chi_{i,j}$  anharmonic coefficients and to extrapolate rotational constants of the excited vibrational states ( $n\nu_i$ ) and ( $n\nu_i + \nu_j$ ).

The energy of the vibrational levels of a molecule whose vibrations are not degenerate is written:

$$E_{\text{vib}} = \sum_i \omega_i \left( \nu_i + \frac{1}{2} \right) + \sum_i \sum_{j \geq i} \chi_{i,j} \left( \nu_i + \frac{1}{2} \right) \left( \nu_j + \frac{1}{2} \right) \quad (2)$$

where  $\omega_i$  are the harmonic frequencies,  $\chi_{i,j}$  the anharmonic corrections (usually negative) and  $\nu_i$ ,  $\nu_j$  the vibrational quantum numbers of modes  $i$  and  $j$ .

The variation in rotational constants can be described by the following equation:

$$X_v = X_e - \sum \alpha_i^X \left( \nu_i + \frac{1}{2} \right) \quad (3)$$

where  $X_e = A_e, B_e, C_e$  are the equilibrium rotational constants,  $X_v = A_v, B_v, C_v$ , the rotational constants in vibrational state  $v$  and  $\alpha_i^X$  the vibration-rotation interaction constants.

For combination states, predicted rotational constants are usually calculated by assuming the additivity of variations in spectroscopic constants as vibrational quantum numbers change, such as  $X_{i+j} = X_i + X_j - X_0$  for the  $i + j \leftarrow 0$  transition. More details can be found in Ref [28].

In the following, the hot band sequences of  $\nu_{27}\mathbf{t}$ ,  $\nu_{26}\mathbf{t}$ ,  $\nu_{26}\mathbf{c}$  and  $\nu_{25}\mathbf{t}$  are analyzed either completely for  $\nu_{27}\mathbf{t}$  or only partially for the other hot bands due to the mixing between upper vibrational states above  $500\text{ cm}^{-1}$ . Each hot transition is introduced progressively according to a set of parameters resulting in a shift in frequency and a change of the rotational band contour : either  $(\chi_{i,i}, X_{(n+1)\nu_i} - X_{n\nu_i} = -\alpha_i^X)$  for the sequences of the type  $(n+1)\nu_i \leftarrow n\nu_i$  or  $(\chi_{i,j}, X_{n\nu_i+\nu_j} - X_{n\nu_i} = -\alpha_j^X)$  for the sequences of the type  $n\nu_i + \nu_j \leftarrow n\nu_i$  depending on whether a single mode  $i$  or two modes  $i$  and  $j$  are involved in the hot band sequence, where  $\alpha_i^X$  is the variation in the rotational constant  $X$  between the GS and the  $\nu_i = 1$  ES. The rovibrational analyses are performed by applying the strict additivity rule for the rotational constants, which allows band contour simulations to be started with realistic sets of rotational constants of the upper states  $(n+1)\nu_i$  or  $\nu_i + \nu_j$ . However, the upper-state rotational constants must be adjusted to reproduce the dense pattern of  ${}^RQ$  and  ${}^PQ$  transitions and, in particular, the frequency positions of intense  ${}^RR$  transitions in two regions. Fig. 8 and 9 display the complete assignment of the *trans*-2-FF hot band sequences,  $(n+1)\nu_{27} \leftarrow n\nu_{27}$  up to  $n=4$ ,  $(n+1)\nu_{26} \leftarrow n\nu_{26}$  up to  $n=2$  and  $\nu_{26} + n\nu_{27} \leftarrow \nu_{26}$  up to  $n=4$ . The rotational band contour of 5 transitions of the  $\nu_{27}$  hot band sequence were simulated individually, then summed to reproduce the Q-branch pattern at room temperature (Fig. 8). Similarly, the first patterns of the double sequence  $(n+1)\nu_{26} \leftarrow n\nu_{26}$  up to  $n=2$ ,  $\nu_{26} + n\nu_{27} \leftarrow \nu_{26}$  up to  $n=3$  have been fully simulated and agree well with the observed spectrum (Fig. 9).

In contrast, the assignment of the hot band sequences linked to the  $\nu_{26}$  mode of *cis*-2-FF is more ambiguous. Compared to the *trans*-2-FF hot band sequence, the  $\nu_{26\mathbf{c}} + n\nu_{27\mathbf{c}} \leftarrow \nu_{26\mathbf{c}}$  transitions are not clearly visible (see Fig. 6). Furthermore, hot-band simulations of the *trans*-2-FF conformer have shown that the evolution of the vibration-rotation interaction constants  $\alpha_i^X$  related to a given hot-band sequence varies little as a function of  $n$ . This is the case of the  $\nu_{27}$  hot band sequence defined as  $(n+1)\nu_{27\mathbf{t}} \leftarrow n\nu_{27\mathbf{t}}$  for which  $\alpha_{27}^X = X_{n\nu_{27\mathbf{t}}} - X_{(n+1)\nu_{27\mathbf{t}}}$ . We obtained  $\alpha_{27}^X$  values equal to 66.4(7), 0.9(6) and 3.1(8) MHz for  $X = \text{A, B, C}$ , respectively (see Table S3 in SupMat4). Conversely, their absolute values differ greatly as a function of mode as evidenced by the measured values of  $\alpha_{26}^X$  equal to 17(4), 1.7(12) and 1.1(1) MHz (see Table S3). In the following, we will exploit the mode dependence of these rovibrational parameters to confirm the assignments of the two red-shifted bands closest to the  $\nu_{26}$  fundamental band. Individual simulations have been carried out which clearly identify that the band red-shifted by  $-2.087\text{ cm}^{-1}$  involves only the  $\nu_{26}$  mode and corresponds to the  $2\nu_{26} \leftarrow \nu_{26}$  transition while that red-shifted by  $-2.639\text{ cm}^{-1}$  also involves the  $\nu_{27}$  mode and corresponds to the  $2\nu_{26} + \nu_{27} \leftarrow \nu_{26} + \nu_{27}$  transition. The two sequences such as  $(n+1)\nu_{26} \leftarrow n\nu_{26}$  and  $(n+1)\nu_{26} + m\nu_{27} \leftarrow n\nu_{26} + m\nu_{27}$  are observed up to  $n=3$  and  $m=2$  (see Fig. 6).

Finally, analysis of the hot-band sequence in the  $\nu_{25}$  band region is also challenging due to band centers of the two conformers being separated by only  $0.08\text{ cm}^{-1}$ , resulting in a partial overlap of the two sequences. Nevertheless, the respective hot-band sequences involving the  $\nu_{27}$  mode could be unambiguously assigned up to  $n=3$ , as displayed in the expanded view in Fig. 7. Table S3 shows the evolution of vibration-rotation interaction constants  $\alpha_i$  along the different hot band sequences identified in the bands  $\nu_{27}\mathbf{t}$ ,  $\nu_{26}\mathbf{t}$ , and  $\nu_{25}\mathbf{t}$ . Table 4 gathers the anharmonic coefficients  $\chi_{i,j}$  and rotational constants measured in these newly identified excited vibrational states from the hot band sequences relative to  $\nu_{27}\mathbf{t}$ ,  $\nu_{26}\mathbf{t}$ ,  $\nu_{26}\mathbf{c}$  and  $\nu_{25}\mathbf{t}$ .

## IV Discussion

### IV-1 Comparison between theoretical and high-resolution results

A total of 9 experimental fundamental frequencies for the two furfural conformers were observed and assigned (see Table 1) on the basis of anharmonic predictions with a mean average error (MAE) of the differences between experimental and calculated values of  $14.8\text{ cm}^{-1}$ , corresponding to a mean relative error of 3.5 %. In particular, the vibrational states involving the  $\nu_{18t}$  mode ( $\nu_{18t}$ ,  $\nu_{18t} + \nu_{26t}$ ) of the *trans* conformer are the most poorly predicted, with deviations of  $-29.3$  and  $-39.6\text{ cm}^{-1}$  respectively (see Fig. 2). Such a large discrepancy could be due to anharmonic resonances with nearby vibrational states. The most probable candidates are the  $\nu_{26t} = 2$  and  $\nu_{26t} = 3$  vibrational states,  $7.5$  and  $9.7\text{ cm}^{-1}$  apart, respectively, from  $\nu_{18t}$  and  $\nu_{18t} + \nu_{26t}$  with same symmetries ( $A'$  for  $\nu_{18t}/2\nu_{26t}$  and  $A''$  for  $\nu_{18t} + \nu_{26t}/3\nu_{26t}$ ). **The 7 remaining fundamental frequencies** were predicted to within 2.4 %, allowing unambiguous vibrational assignments. If we now consider the 22 vibrational energy levels derived from IR and mmW analyses of the fundamental and hot bands (15 for *trans*- and 7 for *cis*-2-FF), the mean average error increases slightly to 3.1 %, **probably due to the higher number of vibrational states (22 vs. 7) taken into account** (see Table S4 in SupMat4).

The calculated GS- and ES-rotational constants for the lowest fundamental frequencies are compared with experimental values for the two 2-FF conformers in Table S5 (SupMat4). They were calculated using Eq. (1) combining two levels of theory. Equilibrium constants were computed using highly correlated *ab initio* methods (CCSD(T)-F12) and a basis set designed for the correlation of both valence and core electrons (CVTZ). Anharmonic vibrational effects, which are less dependent on electron correlation than first-order parameters, were computed with MP2/AVTZ after performing test with different basis sets and different DFT methods. The MAE of the differences ( $\delta = \text{exp} - \text{calc}$ ) between the experimental and calculated rotational constants is equal to 2.9 MHz for *trans*-2-FF and 1.5 MHz for *cis*-2-FF over 15 and 12 constants, respectively. After correction of the calculated values using the GS deviation, the MAEs of the corrected values amounts to 3.2 MHz for *trans*-2-FF and lowers to 1.3 MHz for *cis*-2-FF, mainly due to the larger deviation of the absolute value of the A rotational constant. These MAE values are globally very close to those obtained for vibrational states of 2-FF in the mid-IR range.<sup>11</sup> However, the MAE for both conformers was considerably reduced to only 130 kHz (630 kHz in the mid-IR range) by considering only the B and C corrected constants (14 ES) which gives good confidence in the predictive power of the CCSD(T)-F12b method to derive reliable corrected rotational constants, as was previously shown for rigid and floppy systems of similar size.<sup>29-31</sup> In addition, to obtain very accurate B and C and less accurate A constants is a common behavior of many molecules with a symmetry plane. The divergences are more significant in the case of the low frequency in-plane  $\nu_{19}$  mode.

After the tests carried out with different basis sets and functionals, we found that, as for the rotational parameters, the MP2/AVTZ method produces vibrational energies a better agreement with the experimental ones. Furfural exhibits many low-frequency vibrational levels whose relative order is well described by the MP2 calculations, although computed vibrational energies and anharmonic constants are not as accurate as the rotational parameters. Surprisingly, divergences for many levels are greater than  $10\text{ cm}^{-1}$  and  $\nu_{19}$ , the lowest energy mode of  $A'$  symmetry, whose theoretical rotational constants are the worst, is the best described with MP2/AVTZ.

Several methods were tried to determine a reliable anharmonicity matrix for 2-FF guided by a comparison with few anharmonic coefficients derived accurately from hot band analyses, each of them involving the ring-CHO torsion LAM ( $\nu_{27}$ ). It turns out that VPT2 failed to reproduce experimental coefficients most probably because rotational constants depend on the cubic force field only, while the

anharmonic constants are derived from both cubic and quartic force fields. Required computed derivatives are obtained numerically using Gaussian software and loss accuracy increases with the degree of the derivative. In addition, although the mode  $\nu_{27}$  (out-of-plane) interconverts the two conformers, they are separated by a barrier of  $\sim 3900\text{ cm}^{-1}$  (CCSD(T)-F12), higher enough to treat both conformers as two different species using VPT2, a theory designed for a single minimum.

A variational model of reduced dimensionality working in internal coordinates, designed for the treatment of large amplitude motions<sup>23</sup>, has been applied in three dimensions from a CCSD(T)-F12 potential energy surface. The model describes well the torsional mode ( $\nu_{27}=148.301\text{ cm}^{-1}$ ) but is less accurate for  $\nu_{19}$  and  $\nu_{26}$ , that cannot be reduced to local modes by assuming a separability of variables. We can conclude that the contribution of electron correlation is probably very important for 2-FF. However, the molecule is too large for use of more accurate (therefore more expensive) *ab initio* methods.

## IV- 2 Anharmonic coefficients

Hot bands analyses allowed us to derive seven anharmonic coefficients  $\chi_{i,j}$  for both conformers with excellent relative accuracy, well below 1 % for those involving the  $\nu_{26}$  and  $\nu_{27}$  modes, around 5 % for those involving the  $\nu_{25}$  mode (see Table 4). The coefficients  $\chi_{25,27}$ ,  $\chi_{26,26}$  and  $\chi_{26,27}$  show consistent values across the two conformers with small variations between 10 and 30%, giving confidence in our band assignments, particularly for the  $\nu_{26}$  hot band sequence of *cis*-2-FF. Less accurate values of anharmonic coefficients have been extracted from low-resolution FT Raman and IR measurements.<sup>7-8</sup> The  $\chi_{27,27}$  coefficient was estimated to  $-0.2\text{ cm}^{-1}$  for *cis*-2-FF by Little *et al.*<sup>7</sup>, but with only 2 hot bands and a low SNR. In our previous mid-IR HR spectroscopy study of furfural,<sup>11</sup> we exploited the medium-resolution FT spectra at 298.15 K by Johnson *et al.*<sup>8</sup> to reconstruct rovibrational cross-sections from high-resolution molecular parameters and by considering the most intense hot bands for which Q branches are clearly visible in the room-temperature spectrum. For example, in the region of the  $\nu_{23}$  ring CH out-of-plane bending and  $\nu_{17}$  C-C-H scissoring modes, main sequences with  $\chi_{i,j} = -0.6$  and  $-0.45\text{ cm}^{-1}$  for  $\nu_{23t}$  and  $\chi_{i,j} = -0.6$  and  $-0.35\text{ cm}^{-1}$  for  $\nu_{17t}$  are clearly observed. Some  $\chi_{i,j}$  values estimated in mid-IR range such as  $-0.45$  and  $-0.35\text{ cm}^{-1}$  are very close to those measured in the far-IR range for the modes  $\nu_{26t}$  and  $\nu_{25t}$  coupled to the lowest frequency  $\nu_{27t}$  mode, respectively at  $-0.43$  and  $-0.28\text{ cm}^{-1}$  but no conclusive assignment is possible, among the lowest frequency modes  $\nu_{27}$ ,  $\nu_{19}$  and  $\nu_{26}$ .

## Conclusion

Taking advantage of far-IR high-resolution FT spectroscopy using SOLEIL synchrotron radiation coupled to a long-path absorption cell and complemented by high level of theory quantum-chemistry anharmonic calculations, 18 new vibrational energy levels for the *trans*- and *cis*-conformers of 2-FF were accurately measured and assigned from rovibrational analysis of the fundamental and hot bands related to ring-CHO torsion ( $\nu_{27}$ ), in-plane bending ( $\nu_{19}$ ), out-of-plane bending ( $\nu_{26}$ ) and ring puckering ( $\nu_{25}$ ) modes. Molecular parameters in 4 (3) excited rovibrational states of the *trans* (*cis*) conformer up to  $600\text{ cm}^{-1}$  and ground-state parameters were globally fitted to 22475 *trans* and 7466 *cis* experimental rotational and rovibrational lines. Once the fundamental bands were assigned and analyzed, the hot band sequences linked to the  $\nu_{27t}$ ,  $\nu_{26t}$ ,  $\nu_{26c}$ ,  $\nu_{25t}$  and  $\nu_{25c}$  modes were identified and analyzed line-by-line. This thorough work enabled the accurate determination of the frequency of highly excited states (inaccessible by mmW spectroscopy at room temperature), of the vibration-

rotation interaction constants  $\alpha_i$  within a hot band sequence, and especially of 7 anharmonic constants  $\chi_{i,j}$  involving these three low frequency modes. Despite several theoretical attempts (VPT2, a variational procedure of reduced dimensionality) to reproduce with the best precision the vibrational energy levels and ultimately the anharmonic constants, it appears that the strong contribution of electron correlation for furfural inhibits the correct prediction of these parameters. Unfortunately, full-dimensional computations of anharmonic properties depending on the quartic force field and using highly correlated ab initio methods, are not suitable given the molecular size of furfural. **Fortunately, the high accuracy of the present computed rotational constants in both the ground state and in the excited vibrational levels, confirms assignments that can be considered for further spectroscopic or atmospheric studies.**

## Supplementary Material

Supplemental information is provided in 4 supplementary files : SupMat1 contains 2 tables S1 and S2 including line assignments, measured frequencies, uncertainties and deviations for trans- and cis-2-FF, respectively. SupMat2 contains three tables : table S3 gathers vibration-rotation interaction constants related to hot band sequences observed as a function of n, table S4 compares vibrational energy levels of both conformers with calculated ones up to 700  $\text{cm}^{-1}$  at the MP2-AVTZ level, Table S5 compares the calculated GS- and ES-rotational constants for the lowest fundamental frequencies of two 2-FF conformers with experimental values. SupMat3-cis for the cis-conformer and SupMat4-trans for the trans -conformer gather the complete set of calculated rovibrational transitions obtained with the SPCAT program. The intensities have been calculated at 298.15 K, considering the rotational partition function derived from the fitted rotation constants and the vibrational induced dipolar moments from anharmonic MP2/AVTZ calculations.

## Funding

This project has received funding from the European Union's Horizon 2020 research and innovation programme under the Marie Skłodowska-Curie grant agreement No 872081". This research was supported by the Agencia Estatal de Investigación of Spain through the grant PID2020-112887GB-I00/AEI/10.13039/501100011033.

This work was supported by the CaPPA project (Chemical and Physical Properties of the Atmosphere) funded by the French National Research Agency (ANR-11-LABX-0005-01) and the ECRIN program supported by the Hauts-de-France Regional Council, the French Ministry of Higher Education and Research and the European Regional Development Fund.

## Acknowledgements

The authors are grateful to SOLEIL and the AILES staff for providing a synchrotron beam under Proposal No. 20211555, and to Jordan A. Claus, Joanna Sobczuk and Colwyn Bracquart for their participation to the FF measurements at SOLEIL

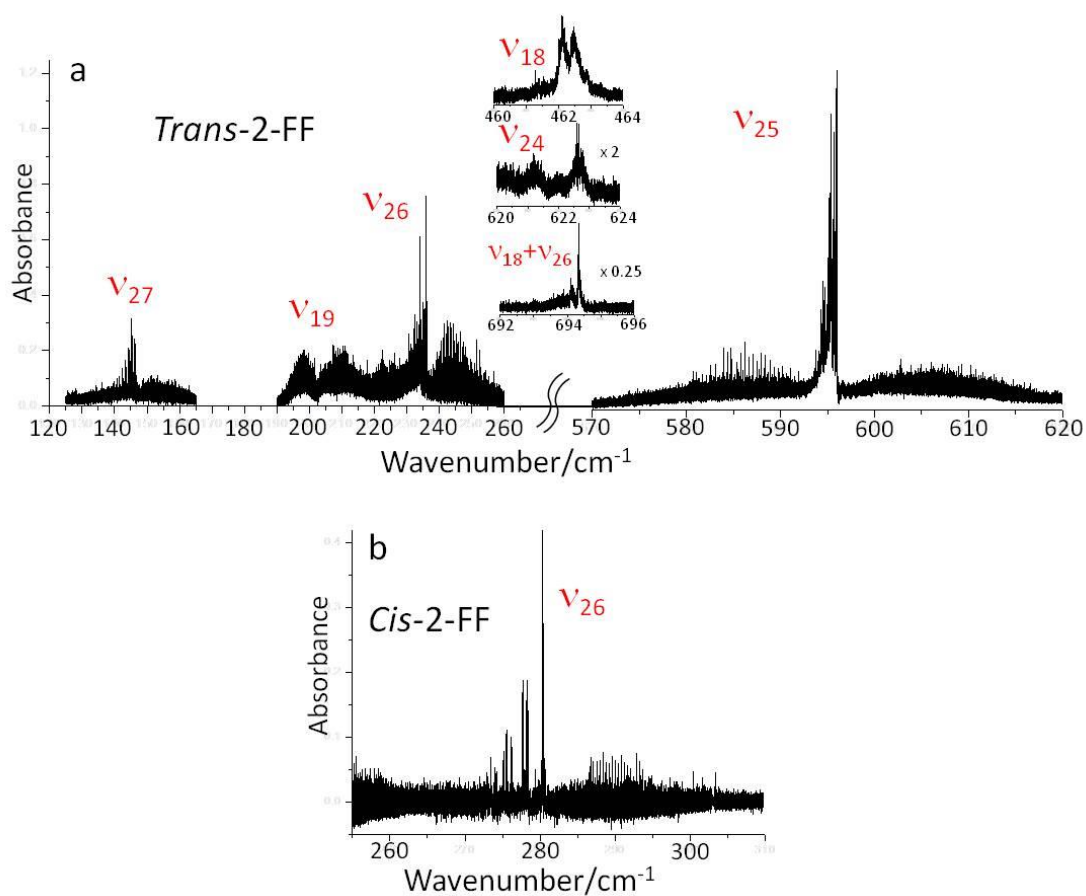


Figure 1: Overview of the high-resolution far-infrared spectra of the two conformers of 2-furfural recorded at a resolution of 0.001 cm<sup>-1</sup> in a 150 m long absorption cell: a) Bands ν<sub>27</sub>, ν<sub>19</sub>, ν<sub>26</sub>, and ν<sub>25</sub> of the *trans* conformer and an enlarged view of the weak bands observed at 462.3, 622.6 and 694.3 cm<sup>-1</sup> assigned respectively to the bands ν<sub>18</sub>, ν<sub>24</sub> and ν<sub>18</sub>+ν<sub>26</sub>, b) the ν<sub>26</sub> band of the *cis* conformer.

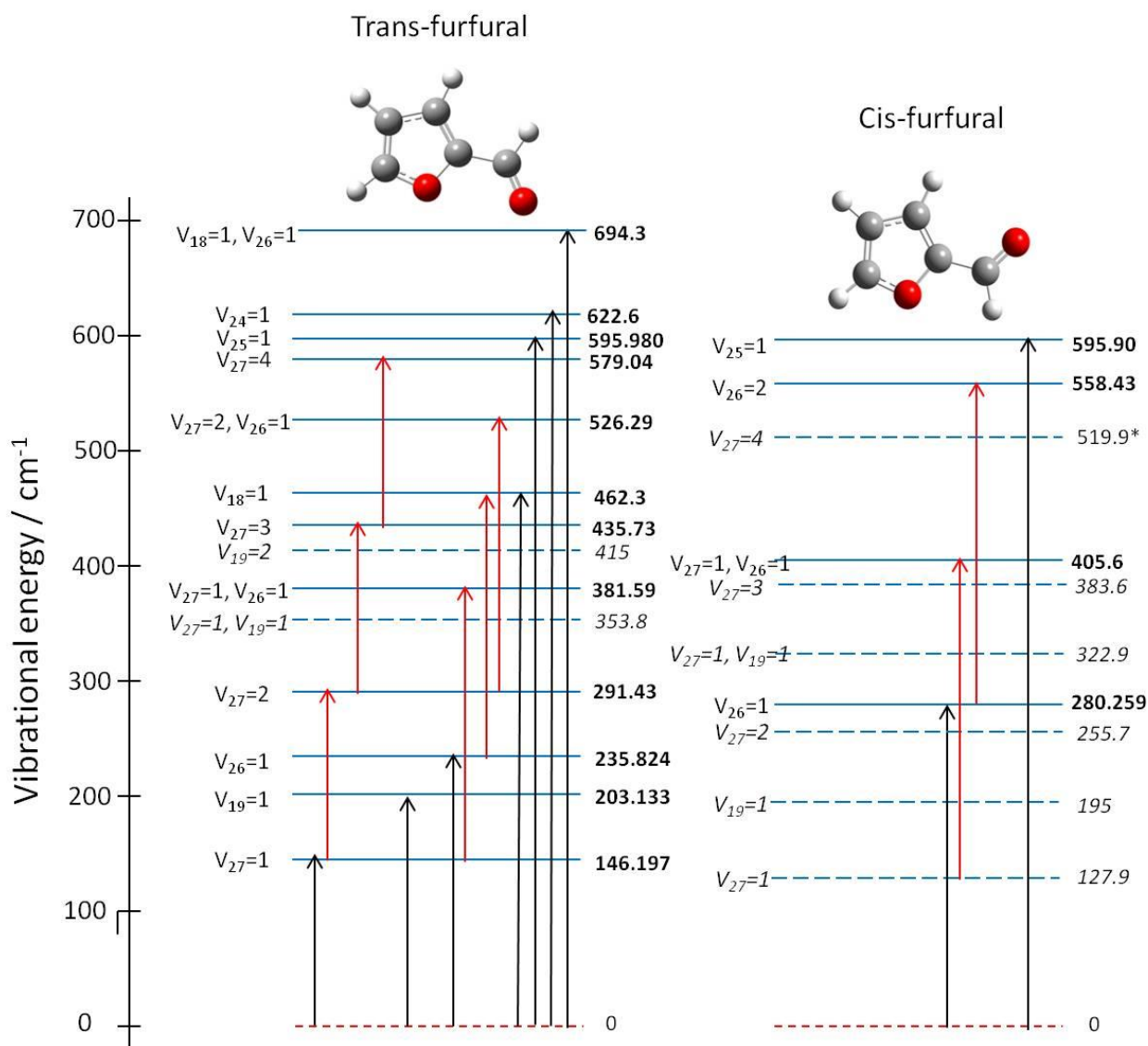


Figure 2: The vibrational energy level scheme of *trans*- and *cis*-conformers of 2-furfural. The labels of vibrational states in italics correspond to states analyzed from previous MW and mmW studies by Motiyenko *et al* (marked by blue dotted lines). Vibrational frequencies of  $v_{27}=1$  and  $v_{19}=1$  of *cis*-2-furfural were measured by Little *et al* [7] and Mönning *et al* [32], respectively. The other labels correspond to 18 vibrational states (marked by solid blue lines) assigned in the present far-IR study: 9 states are reached by fundamental, overtone and combination transitions starting from the GS (black arrow), 9 by hot transitions starting from an ES (red arrow). The energy level value marked with an asterisk was computed using the MP2/AVTZ method.

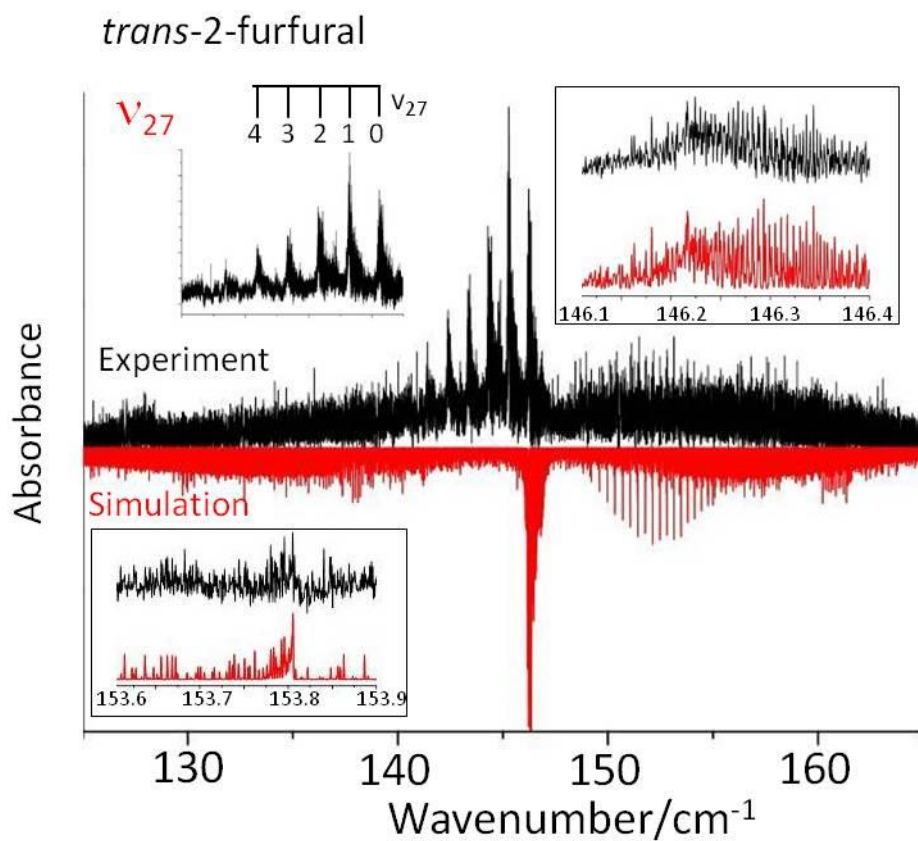


Figure 3: Comparison between the experimental  $\nu_{27}$  band of *trans*-2-furfural (black) and the simulation of the  $\nu_{27} = 1 \leftarrow 0$  transition at  $T = 300$  K (red). Two expanded views display the resolved rotational structure of the R-branch (bottom left) and the Q-branch (top right). A third expanded view displays the hot band sequence  $(n + 1)\nu_{27} \leftarrow n\nu_{27}$  up to  $n = 4$  (top left) on the P-branch side.

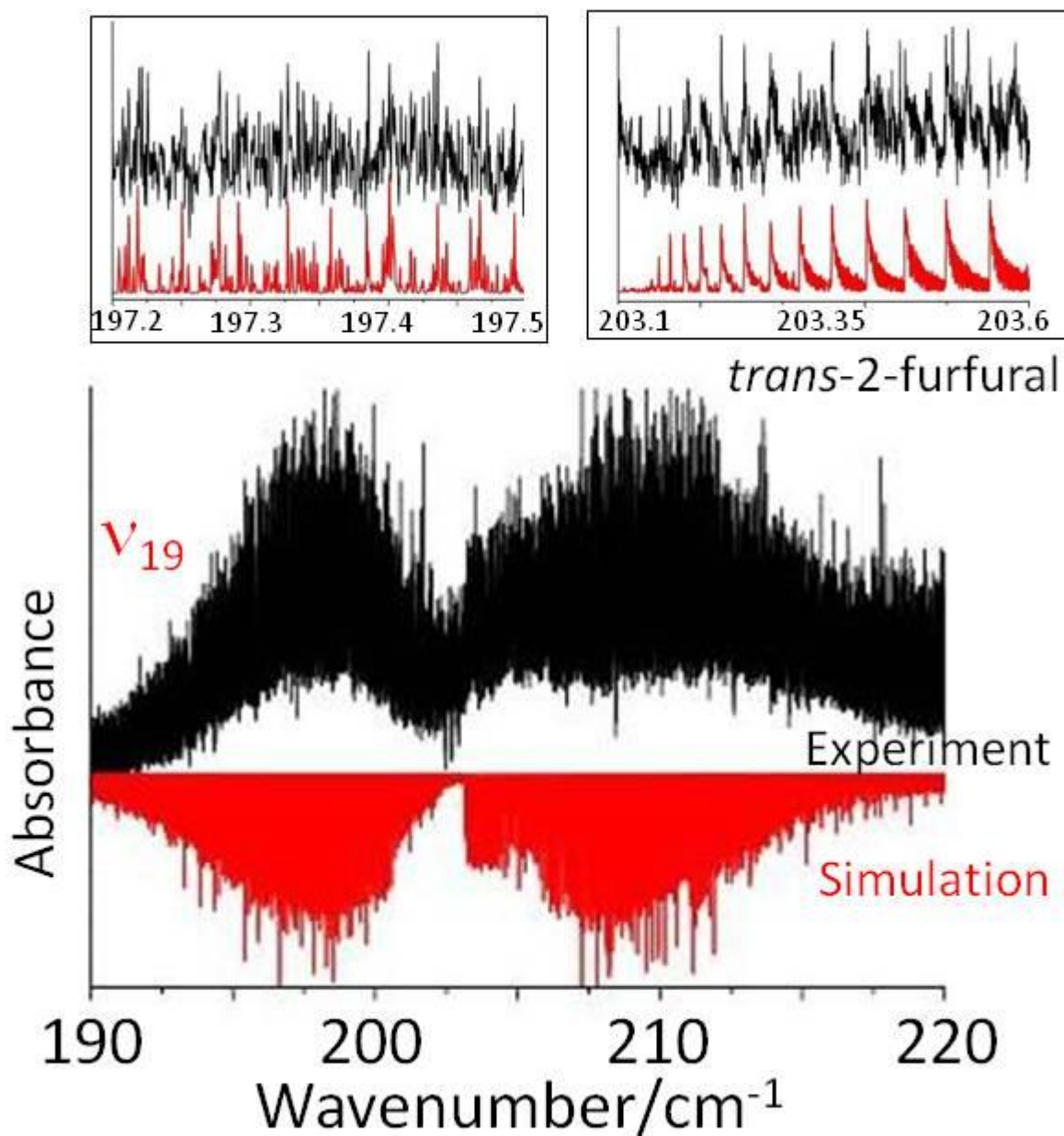


Figure 4: Comparison between the experimental  $\nu_{19}$  band of *trans*-2-furfural (black) and the simulation of the  $\nu_{19}=1\leftarrow 0$  transition at  $T=300$  K (red). The two expanded views display the resolved rotational structure of the P-branch (top left) and a detail of the Q-branch pattern (top right). **No hot band sequence is observed for the b-type  $\nu_{19}$  band.**

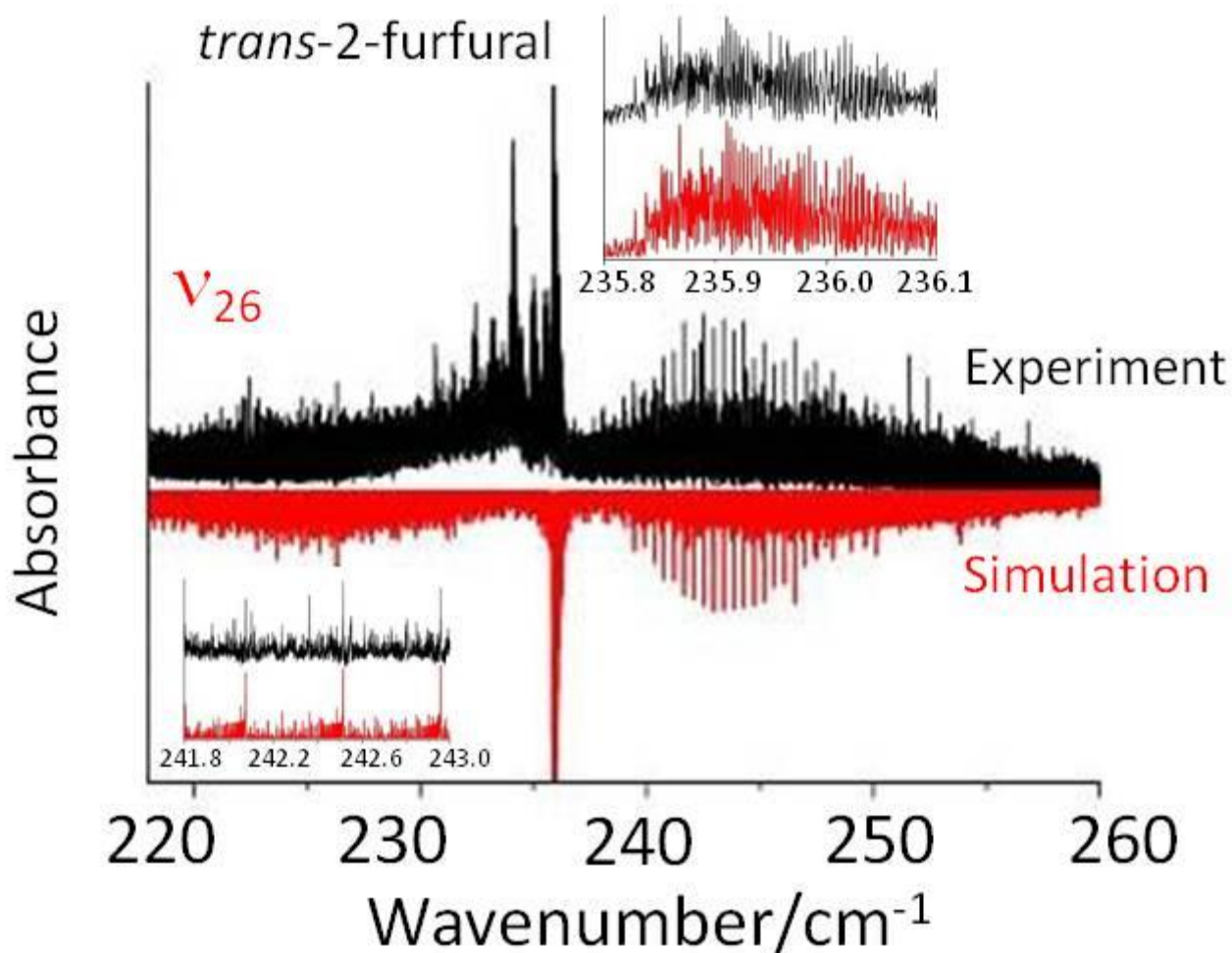


Figure 5: Comparison between the experimental  $\nu_{26}$  band of *trans*-2-furfural (black) and the simulation of the  $\nu_{26}=1\leftarrow 0$  transition at T=300 K (red). The two expanded views display the resolved rotational structure of the R-branch (bottom left) and the Q-branch (top right). An irregular hot band pattern is observed on the red side of the  $\nu_{26}=1\leftarrow 0$  transition, suggesting two sequences involving ring-CHO torsion ( $\nu_{27}$ ) and out-of-plane bending ( $\nu_{26}$ ) modes.

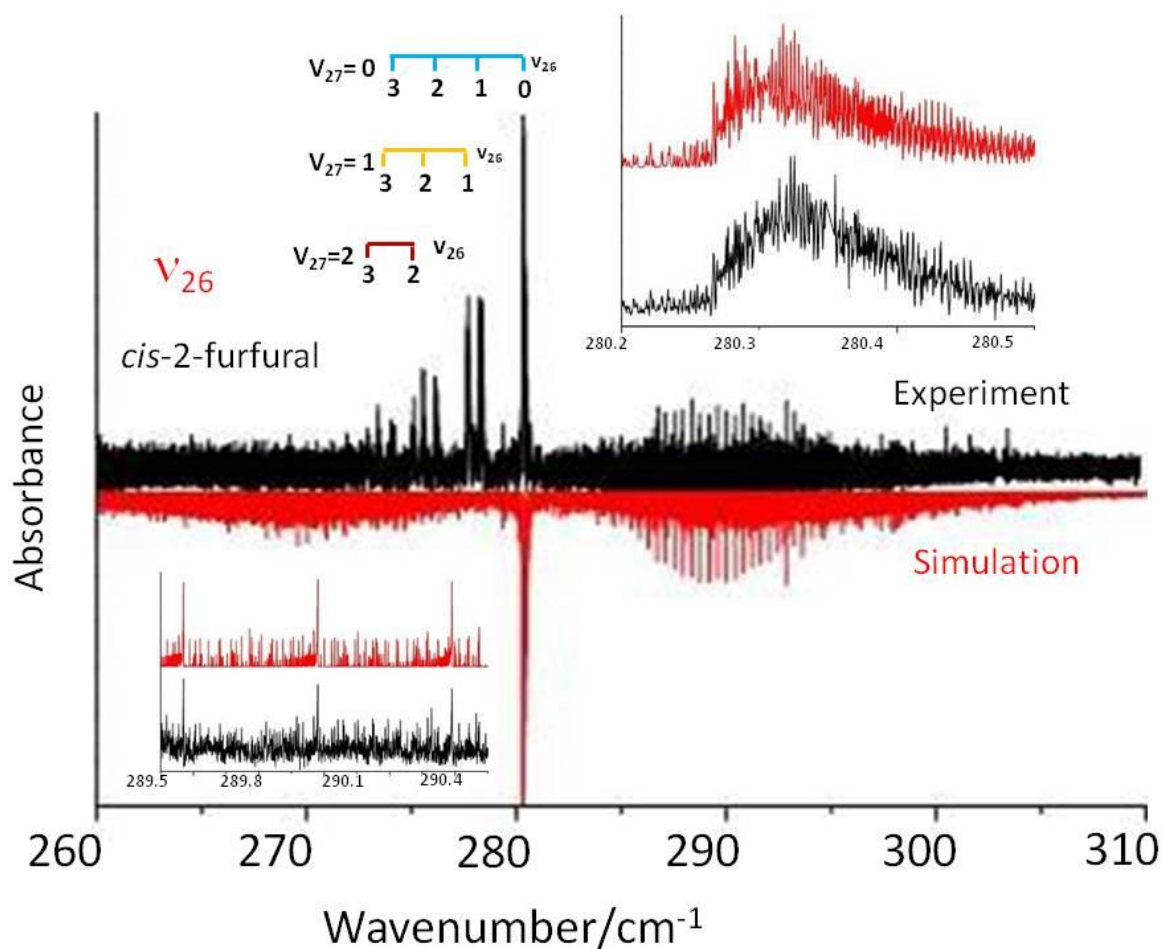


Figure 6: Comparison between the experimental  $\nu_{26}$  band of *cis*-2-furfural (black) and the simulation of the  $\nu_{26}=1\leftarrow 0$  transition at  $T=300\text{ K}$  (red). The two expanded views display the resolved rotational structure of the R-branch (bottom left) and the Q-branch (top right). The assignment of the complex pattern of hot bands involving modes  $\nu_{26}$  and  $\nu_{27}$  is displayed on the red side of the fundamental band.

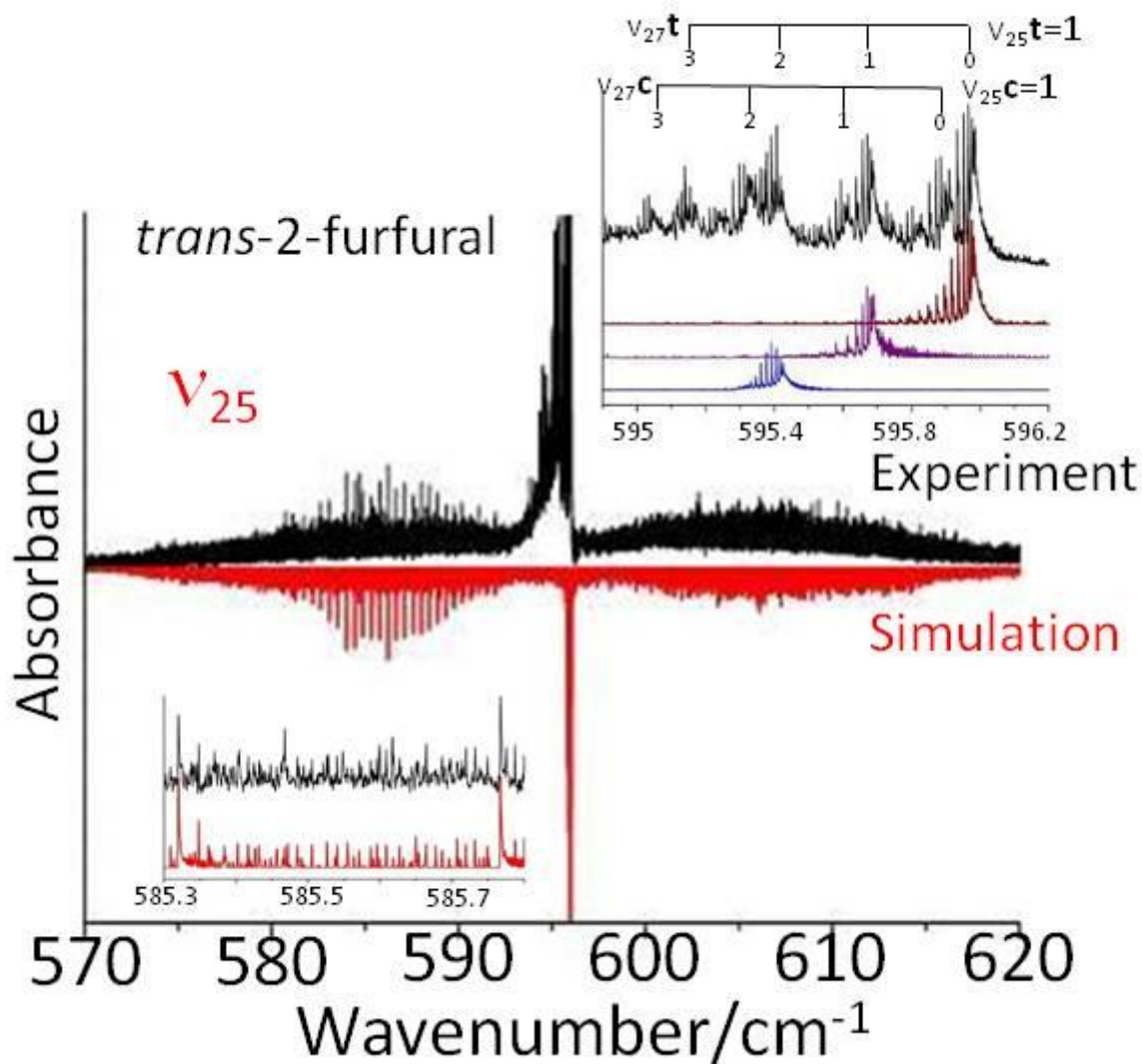


Figure 7: Comparison between the experimental  $\nu_{25}$  band of *trans*-2-furfural (black) and the simulation of hot band sequences involving  $\nu_{25}\mathbf{t} + n\nu_{27}\mathbf{t} \leftarrow n\nu_{27}\mathbf{t}$  and  $\nu_{25}\mathbf{c} + n\nu_{27}\mathbf{c} \leftarrow n\nu_{27}\mathbf{c}$  up to  $n=3$  at  $T=300$  K (red). The bottom left expanded view displays the resolved rotational structure of the P-branch. The top right expanded view displays two hot band sequences of  $\nu_{25}\mathbf{t}$  and  $\nu_{25}\mathbf{c}$  conformers involving the lowest frequency  $\nu_{27}$  mode in the Q-branch region.

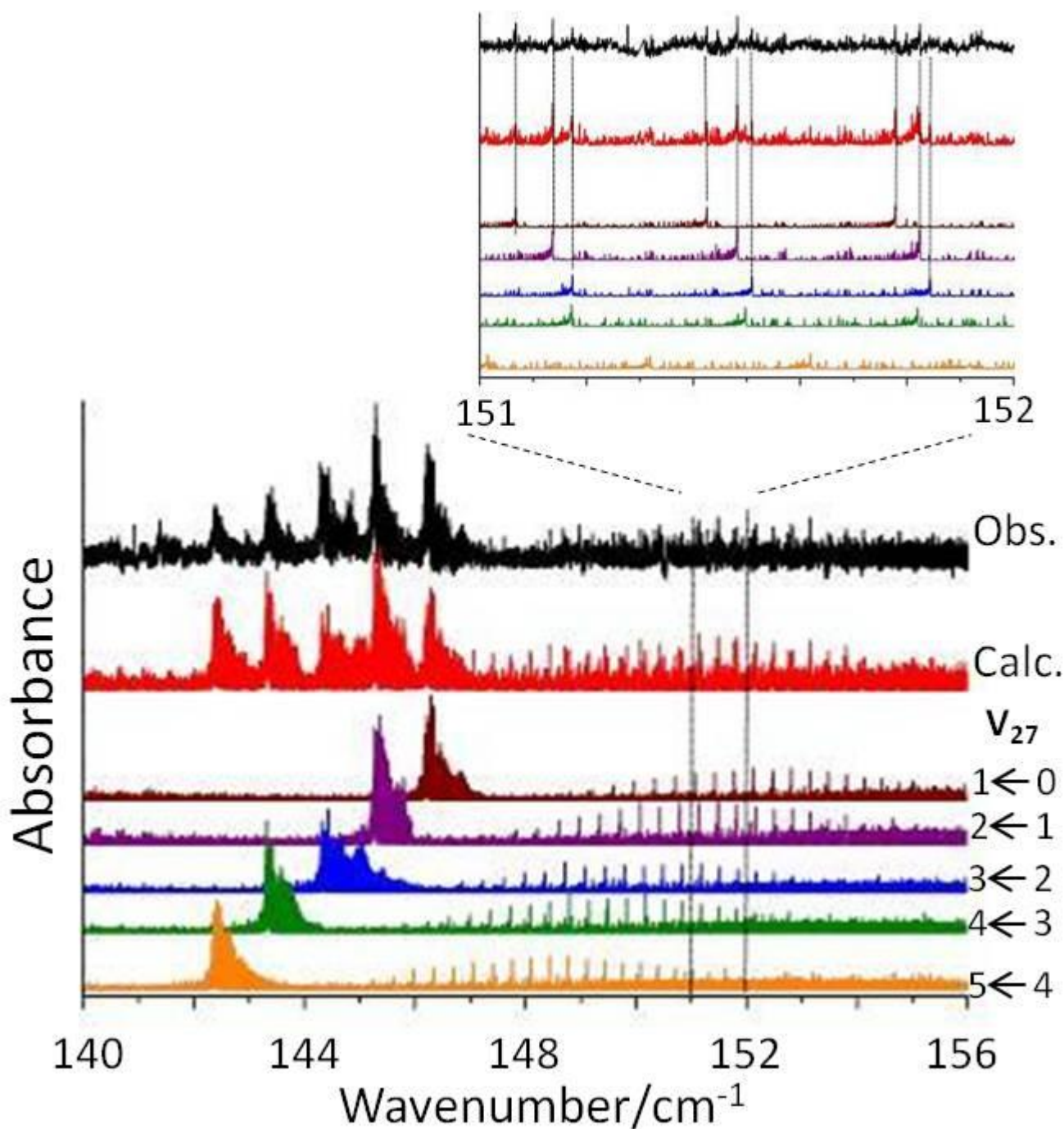


Figure 8: Overview of the Q-branch hot band pattern and R-branch of the  $\nu_{27}$  band of *trans*-2-furfural at 300 K (black) compared with the simulated spectrum composed of 5 transitions  $(n + 1)\nu_{27} \leftarrow n\nu_{27}$  up to  $n = 4$  (red). Each transition of the sequence, shifted by about  $-0.96 \text{ cm}^{-1}$  from the next one, is displayed. An expanded view of the R-branch in the  $151\text{-}152 \text{ cm}^{-1}$  region shows the assignments of  $^{\text{R}}\text{R}$  hot band transitions (in purple, blue, green, orange) shifted from the fundamental band (maroon).

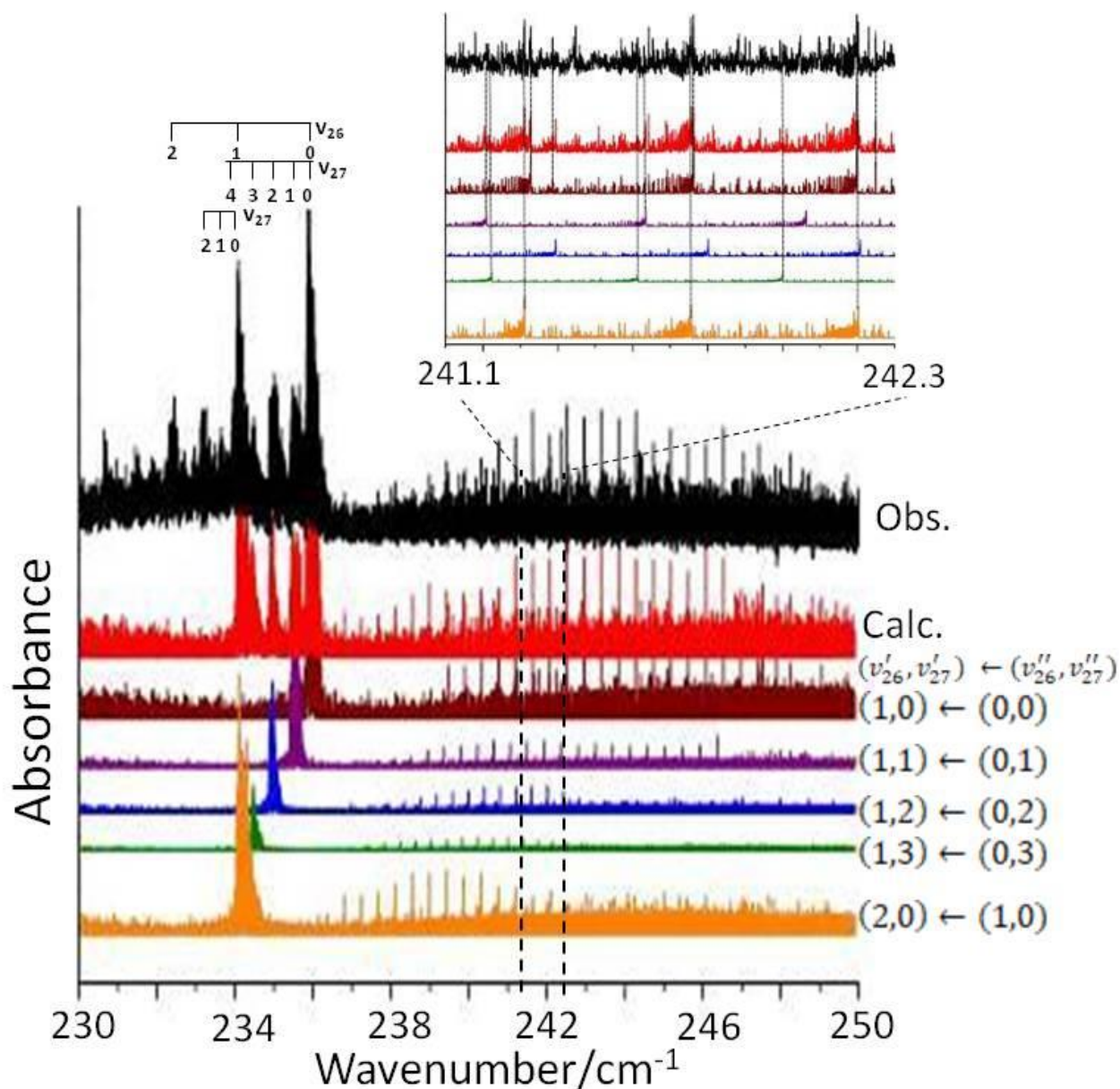


Figure 9: Overview of the Q-branch hot band pattern and R-branch of the  $\nu_{26}$  band of *trans*-2-furfural at 300 K (black) compared with the simulated spectrum composed of 5 transitions, 2 belonging to the hot band sequence  $(n+1)\nu_{26} \leftarrow n\nu_{26}$  up to  $n=1$ , shifted by about  $-1.81 \text{ cm}^{-1}$ , and 3 to the hot band sequence  $\nu_{26} + n\nu_{27} \leftarrow \nu_{26}$  up to  $n=3$ , shifted by about  $-0.86 \text{ cm}^{-1}$  (red). An expanded view of the R-branch in the 241.1-242.3  $\text{cm}^{-1}$  region shows the assignments of RR hot band transitions (in purple, blue, green, orange) shifted from the fundamental band (maroon).

$\nu_{\text{exp}}$ (FIR)	$\nu_{\text{exp}}^{\text{a}}$	Mode	symmetry	conformer	$\nu_{\text{MP2/AVTZ}}$	Description
694.3		$\nu_{18}+\nu_{26}$	A''	trans	735.9	
622.6		$\nu_{24}$	A''	trans	635.2	ring puckering
595.97994		$\nu_{25}$	A''	trans	609.9	ring puckering
595.9		$\nu_{25}$	A''	cis	610.0	ring puckering
462.3		$\nu_{18}$	A'	trans	491.6	
280.25936	280.2	$\nu_{26}$	A''	cis	288.3	ring CHO oop
235.82428	235.9	$\nu_{26}$	A''	trans	247.5	ring CHO oop
203.13242	212.4	$\nu_{19}$	A'	trans	203.2	ring CHO ip
146.19761	146.25	$\nu_{27}$	A''	trans	148.7	ring CHO torsion

<sup>a</sup>Little *et al* [7].

Table 1: 2-furfural vibrational far-IR assignments based on our experimental measurements compared with mmW energy level measurements, as well as anharmonic calculations at the MP2/AVTZ level. All vibrational frequencies are given in  $\text{cm}^{-1}$  unit.

Frequency ( $\text{cm}^{-1}$ )	GS	$\nu_{27}$ 146.197611(8)	$\nu_{19}$ 203.132423(8)	$\nu_{26}$ 235.824278(9)	$\nu_{25}$ 595.979939(11)
A	8191.77320(28)	8115.4201(15)	8248.4062(19)	8205.7582(24)	8176.9316(18)
B	2045.929560(18)	2045.58344(4)	2047.62616(8)	2046.5305(16)	2044.8710(12)
C	1637.183892(18)	1639.62750(4)	1636.98563(6)	1638.2701(12)	1637.4168(18)
$\Delta_{\text{J}}(\times 10^3)$	0.1361878(83)	0.137661(13)	0.134265(27)	0.13706(11)	0.14374(27)
$\Delta_{\text{K}}(\times 10^3)$	1.7763(17)	1.0324(31)	5.1582(38)	1.1996(53)	1.8420(28)
$\Delta_{\text{JK}}(\times 10^3)$	0.706640(41)	0.54488(8)	0.94454(38)	0.6214(8)	0.6517(17)
$\delta_{\text{J}}(\times 10^6)$	0.0314665(40)	0.031535(6)	0.030982(17)	0.03141(3)	0.03480(15)
$\delta_{\text{K}}(\times 10^6)$	0.82181(31)	0.42902(60)	1.0639(9)	0.9619(46)	1.3499(14)
$\Phi_{\text{J}}(\times 10^9)$	-0.0178(16)	0.0200(22)	0.0186(27)	0.293(39)	<i>-0.0178</i>
$\Phi_{\text{JK}}(\times 10^9)$	0.645(78)	-4.71(12)	-1.09(53)	21.0(14)	<i>0.645</i>
$\Phi_{\text{KJ}}(\times 10^9)$	-5.03(27)	-16.19(44)	15.7(22)	-66.8(66)	<i>-5.03</i>
$\phi_{\text{J}}(\times 10^{12})$	8.39(54)	8.64(80)	8.39	8.39	8.39
$\phi_{\text{K}}(\times 10^9)$	13.1(17)	-94.2(26)	68.1(111)	373(31)	<i>13.1</i>
$\phi_{\text{JK}}(\times 10^9)$	0.402(52)	-0.193(85)	<i>0.402</i>	4.1(16)	<i>0.402</i>
$L_{\text{J}}(\times 10^{15})$	0.168(92)	<i>0.168</i>	<i>0.168</i>	-22(3)	<i>0.168</i>
$L_{\text{KKJ}}(\times 10^{12})$	-0.110(14)	2.835(32)	-7.64(94)	12.8(17)	<i>-0.110</i>
Mw(IR) RMS	0.008	0.009(4.9)	0.008(4.8)	0.008(4.0)	(4.8)
N lines	1844	4342	5424	5697	5184
$J''$	1-99	1-99	1-99	1-96	0-99
$K''_{\text{a}}$	0-53	0-48	0-40	0-41	1-36

Table 2: Molecular parameters (in MHz) of the ground state,  $\nu_{27}=1$ ,  $\nu_{19}=1$ ,  $\nu_{26}=1$ , and  $\nu_{25}=1$  of *trans*-2-furfural derived from the global fit of rotational lines in the  $\nu=0$ ,  $\nu_{27}=1$ ,  $\nu_{19}=1$ ,  $\nu_{26}=1$  states from the mmW study<sup>10</sup> and rovibrational lines of the  $\nu_{27}$ ,  $\nu_{19}$ ,  $\nu_{26}$ , and  $\nu_{25}$  bands from our far-IR study. The ES quartic, sextic and octic parameters in italics were fixed to the GS value for the global fit.

Frequency (cm <sup>-1</sup> )	GS	v <sub>27</sub> 127.86 <sup>a</sup>	v <sub>19</sub> 195 <sup>b</sup>	v <sub>26</sub> 280.259363(10)
A	8143.73873(72)	8077.8111(16)	8201.813(11)	8139.1325(16)
B	2098.724249(17)	2099.57613(20)	2100.04789(26)	2098.79476(15)
C	1668.872904(17)	1672.04780( 8)	1668.18781(13)	1669.80184(10)
Δ <sub>J</sub> (x10 <sup>3</sup> )	0.172659(7)	0.174913(64)	0.169573(88)	0.17293(4)
Δ <sub>K</sub> (x10 <sup>3</sup> )	1.81402(24)	0.1584( 83)	3.66(19)	1.8584(17)
Δ <sub>JK</sub> (x10 <sup>3</sup> )	0.49995(4)	0.46107(31)	0.53757( 62)	0.48702( 44)
δ <sub>J</sub> (x10 <sup>6</sup> )	0.040304(5)	0.040386( 35)	0.039505( 44)	0.040288(24)
δ <sub>K</sub> (x10 <sup>6</sup> )	0.80894(23)	0.6002(17)	1.0130(31)	0.8206(16)
Φ <sub>J</sub> (x10 <sup>9</sup> )	0.0271(11)	<i>0.0271</i>	0.0186(27)	<i>0.271</i>
Φ <sub>JK</sub> (x10 <sup>9</sup> )	-0.3226(75)	-0.30(15)	-0.32(25)	-0.48(12)
Φ <sub>KJ</sub> (x10 <sup>9</sup> )	-2.261(27)	-5.79(25)	1.55( 56)	-0.75(56)
φ <sub>J</sub> (x10 <sup>12</sup> )	10.83(79)	<i>10.83</i>	<i>10.83</i>	<i>10.83</i>
φ <sub>JK</sub> (x10 <sup>9</sup> )	0.139(46)	<i>0.139</i>	<i>0.139</i>	<i>0.139</i>
mw(IR) RMS	0.012	0.011	0.009	0.012(4)
N lines	2488	310	284	4113
J''	1-89	1-47	1-43	0-99
K'' <sub>a</sub>	0-48	0-36	0-31	0-37

Little *et al* [7]. <sup>b</sup>Mönnig *et al* [32].

Table 3: Molecular parameters (in MHz) of the ground state, v<sub>26</sub>=1, of *cis*-2-furfural derived from the global fit of rotational lines in the v=0, v<sub>27</sub>=1, v<sub>19</sub>=1, v<sub>26</sub>=1 states from the mmW study<sup>10</sup> and rovibrational lines of the v<sub>26</sub>, band from our far-IR study and *ab initio* CCSD(T)-F12 rotational constants (in italics). The ES quartic, sextic and octic parameters in italics were fixed to the GS value for the global fit. The ES parameters in italics were fixed to the GS value for the global fit.

	26t	27t
25t		-0.278(14)
26t	-0.900(5)	-0.437(2)
27t		-0.482(1)

	26c	27c
25c		-0.26(2)
26c	-1.045(5)	-0.55(1)
27c		-0.2 <sup>a</sup>

<sup>a</sup>Little *et al* [7]

Table 4: Experimental anharmonic vibrational coefficients (in cm<sup>-1</sup>) of *trans*- and *cis*-2-furfural determined from the rovibrational hot band analysis of our far-IR spectroscopic study.

## References

- <sup>1</sup> X. Jiang, N. T. Tsona, L. Jiu, S. Liu, H. Zhang, Y. Xu and L. Du, *Atmos. Chem. Phys.* **19**, 13591 (2019).
- <sup>2</sup> M. Perzon, *Biomass and Bioenergy*, **34**, 828 (2010).
- <sup>3</sup> J. D. Mc Donald, B. Zielinska, E. M. Fujita, J. C. Sagebiel, J. C. Chow and J. G. Watson, *Environ. Sci. Technol.* **34**, 2080 (2000).
- <sup>4</sup> X. Zhao, L. Wang, *J. Phys. Chem. A*. **121**, 3247 (2017).
- <sup>5</sup> F. Al Ali, C. Cœur, N. Houzel, P. Genevray, F. Cazier, A. Cuisset, V.C. Papadimitriou, A. Tomas and M. N. Romanias. *Atmospheric Environment*, **319**, 120276 (2024).
- <sup>6</sup> J. Decker, E. Fertein, J. Bruckhuisen, N. Houzel, P. Kulinski, B. Fang, W. Zhao, F. Hindle, G. Dhont, R. Bocquet, G. Mouret, C. Coeur and A. Cuisset, *Atmospheric Measurement Techniques*, **15** (5), 1201 (2022).
- <sup>7</sup> T.S. Little, J. Qiu and J.R. Durig, *Spectrochim. Acta Part A Mol. Spectrosc.*, **45**, 789 (1989).
- <sup>8</sup> T.J. Johnson, L.T.M. Profeta, R.L. Sams, D.W.T Griffith and R.L. Yokelson, *Vib. Spectrosc.* **53**, 97 (2010).
- <sup>9</sup> R.A. Motiyenko, E.A. Alekseev, S.F. Dyubko and F.J. Lovas, *J. Mol. Spectrosc.* **240**, 93 (2006).
- <sup>10</sup> R.A. Motiyenko, E.A. Alekseev, S.F. Dyubko *J. Mol. Spectrosc.* **244**, 9 (2007).
- <sup>11</sup> S. Chawananon, P. Asselin, J.A. Claus, M. Goubet, A. Roucou, R. Georges, J. Sobczuk, C. Bracquart, O. Pirali and A. Cuisset, *Molecules* **28**, 4165 (2023).
- <sup>12</sup> I. Gordon, L. Rothman, R. Hargreaves, R. Hashemi, E. Karlovets, F. Skinner, E. Conway, C. Hill, R. Kochanov, Y. Tan et al. *J. Quant. Spectrosc. Radiat. Transf.* **277**, 107949 (2022).
- <sup>13</sup> I. Smirnova, A. Cuisset, F. Hindle, G. Mouret, R. Bocquet, O. Pirali and P. Roy, *J. Phys. Chem. B* **114**, 1693 (2010).
- <sup>14</sup> V.-M. Horneman, R. Anttila, S. Alanko and J. Pietila, *J. Mol. Spectr.* **234**, 238 (2005).
- <sup>15</sup> G. Knizia, T. B. Adler and H.-J Werner, *J. Chem. Phys.* **130**, 054104 (2009).
- <sup>16</sup> T. B. Adler, G. Knizia and H.-J. Werner, *J. Chem. Phys.* **127**, 221106, (2007).
- <sup>17</sup> MOLPRO, version 2022, a package of ab initio programs, H.-J. Werner, P. J., Knowles and others, see <https://www.molpro.net>.
- <sup>18</sup> D.E.Woon and T.H. Dunning, *J. Chem. Phys.*, **103**, 4572 (1995).
- <sup>19</sup> V. Barone, *J. Chem. Phys.* **122**, 014108 (2005).
- <sup>20</sup> M.J. Frisch, G.W. Trucks, H.B. Schlegel, G.E. Scuseria, M.A. Robb, J.R. Cheeseman, G. Scalmani, V. Barone, G.A. Petersson, H. Nakatsuji et al, Gaussian 16, Revision, C.01; Gaussian, Inc.: Wallingford, CT, USA, (2016).
- <sup>21</sup> C. Møller, and M. S. Plesset, *Phys. Rev.* **46**, 618 (1934).
- <sup>22</sup> R.A Kendall, T.H. Dunning Jr and R.J. Harrison, *J. Chem. Phys.*, **96**, 6796 (1992).
- <sup>23</sup> H. Louis, T.C. Egemonye, T.O. Unimuke, B.E. Inah, H.O. Edet, E.A. Eno, S. A. Adalikwu and A.S. Adeyinka, *ACS Omega*, **7**, 34929 (2022).
- <sup>24</sup> S. Grimme, *Wiley Interdiscip Rev Comput Mol Sci*, **1**, 211 (2011).
- <sup>25</sup> R. Boussassi and M.L. Senent, *Phys. Chem. Chem. Phys.* **22**, 23785 (2020).
- <sup>26</sup> C.M. Western, *J. Quant. Spectrosc. Radiat. Transfer* **186**, 221 (2017).
- <sup>27</sup> H. M. Pickett, *J. Mol. Spectrosc.* **148**, 371 (1991).
- <sup>28</sup> J.M. Hollas, *High Resolution Spectroscopy*, John Wiley & Sons (1998).
- <sup>29</sup> S. Gruet, O. Pirali, M. Goubet, D. W. Tokaryk and P. Brechignac, *J. Phys. Chem. A*, **120**, 95 (2016).
- <sup>30</sup> S. Bteich, M. Goubet, R. Motiyenko, L. Margulès and T. Huet, *J. Mol. Spectrosc.* **348**, 124 (2018).
- <sup>31</sup> A. Roucou, A., M. Goubet, I. Kleiner, S. Bteich and A. Cuisset, *ChemPhysChem*. **21**, 2523 (2020).
- <sup>32</sup> F. Mönnig, H. Dreizler and H. D. Rudolph, *Z. Naturf.* **20a**, 1323 (1966).